Journal of Biomechanics 159 (2023) 111777

Contents lists available at ScienceDirect

Journal of Biomechanics

journal homepage: www.elsevier.com/locate/jbiomech

Hemodynamic effects of a dielectric elastomer augmented aorta on aortic wave intensity: An *in-vivo* study

Silje Ekroll Jahren [a,b,*], Thomas Martinez [a], Armando Walter [a], Lorenzo Ferrari [a,b], Francesco Clavica [a,b], Dominik Obrist [b], Yoan Civet [a], Yves Perriard [a]

[a] *Integrated Actuators Laboratory (LAI), École polytechnique fédérale de Lausanne (EPFL), Neuchâtel, Switzerland*
[b] *ARTORG Center for Biomedical Engineering Research, University of Bern, Bern, Switzerland*

ARTICLE INFO

Keywords:
Wave intensity analysis
Aortic counterpulsation
Cardiac assist device
Arterial hemodynamics

ABSTRACT

Dielectric elastomer actuator augmented aorta (DEA) represents a novel approach with high potential for assisting a failing heart. The soft tubular device replaces a section of the aorta and increases its diameter when activated. The hemodynamic interaction between the DEA and the left ventricle (LV) has not been investigated with wave intensity (WI) analysis before. The objective of this study is to investigate the hemodynamic effects of the DEA on the aortic WI pattern. WI was calculated from aortic pressure and flow measured *in-vivo* in the descending aorta of two pigs implanted with DEAs. The DEAs were tested for different actuation phase shifts (PS). The DEA generated two decompression waves (traveling upstream and downstream of the device) at activation followed by two compression waves at deactivation. Depending on the PS, the end-diastolic pressure (EDP) decreased by 7% (or increased by 5–6%). The average early diastolic pressure augmentation ($\overline{P_{dia}}$) increased by 2% (or decreased by 2–3%). The hydraulic work (W_H) measured in the aorta decreased by 2% (or increased by 5%). The DEA-generated waves interfered with the LV-generated waves, and the timing of the waves affected the hemodynamic effect of the device. For the best actuation timing the upstream decompression wave arrived just before aortic valve opening and the upstream compression wave arrived just before aortic valve closure leading to a decreased EDP, an increased $\overline{P_{dia}}$ and a reduced W_H.

1. Introduction

Aortic counterpulsation devices (ACPs) are used to assist and unload the cardiovascular system especially in high-risk patients with acute cardiovascular disease (De Waha et al., 2014; Santa-Cruz et al., 2006). The ACP concept is to reduce the left ventricular afterload to unload the left ventricle (LV) and augment the early diastolic pressure to enhance coronary flow. ACPs can be either intra-aortic (De Waha et al., 2014; Santa-Cruz et al., 2006), para-aortic (Lu et al., 2011) or extra-aortic (Campos Arias et al., 2017; Davies et al., 2005). The intra-aortic balloon pump (IABP) is the most widely used ACP. However, IABP patients may suffer from serious complications (De Waha et al., 2014; Khan et al., 2023; Santa-Cruz et al., 2006), and pneumatic actuation might lead to unpredictable actuation delays (Bruti et al., 2015).

An *augmented aorta* based on a dielectric elastomer actuator (DEA) is a soft tubular cardiac assist device with purely electrical actuation (Almanza et al., 2021) suggested for ACP (Martinez et al., 2022). DEAs consist of a dielectric membrane placed between compliant electrodes. By applying a voltage between the electrodes, the dielectric membrane is compressed in the thickness direction and expanding in all other directions (Pelrine et al., 2000). The soft DEA (distensibility: $2{\cdot}10^{-3}$ mmHg^{-1}, pulse wave velocity (PWV): 7.9 m/s) replaces an aortic section (distensibility: $2.5{\cdot}10^{-3} - 4.5{\cdot}10^{-3}$ mmHg^{-1}, PVW: 3.5 – 11 m/s (Redheuil et al., 2010)) and actively increases and decreases its diameter in response to voltage. The change in diameter is a result of the applied voltage and the internal pressure in the tube (Martinez et al., 2022). The purely electrical actuation, the lightweight, and the non-obstructive nature of the DEA are advantages compared to current ACPs. It might be possible to fully implant and power the DEA with trans-cutaneous wireless power transfer (Knecht et al., 2015). The non-obstructive DEA could be actuated at any time during the heart cycle to optimize the assistance. A detailed comparison of the DEA with other ACPs can be found in (Martinez et al., 2022).

Wave intensity analysis (WIA) uses the simultaneous measurement

* Corresponding author at: ARTORG Center for Biomedical Engineering Research, Cardiovascular Engineering, Freiburgstrasse 3, 3010 Bern, Switzerland.
E-mail address: silje.jahren@unibe.ch (S.E. Jahren).

https://doi.org/10.1016/j.jbiomech.2023.111777
Accepted 22 August 2023
Available online 25 August 2023

of pressure and flow velocity to study arterial wave propagation (Khir et al., 2001b; Parker, 2009). The wave intensity (WI) pattern in arteries typically consist of two forward traveling waves: one compression wave (FCW) at start of systole (created by blood ejection) and one decompression wave (FDW) at end of systole (created by blood flow deceleration). WIA has been used to study arterial hemodynamics (Sun et al., 2000) and the effect of cardiovascular diseases, surgery (Khir et al., 2001a; Sugawara et al., 2009), and drugs (Penny et al., 2008), and to analyze the impact and performance of ACPs (Campos Arias et al., 2017; Kolyva et al., 2009; Lu et al., 2012) and pulsatile ventricular assist devices (PVADs) (Jahren et al., 2014; Khir et al., 2006). Kolyva et al., 2009 identified two pairs of waves caused by the IABP. The inflation resulted in a backward traveling compression wave (BCW) and its reflected FCW which correlates with the pressure augmentation. The deflation resulted in a backward traveling decompression wave (BDW) and its reflected FDW which correlates with the decrease of end-diastolic pressure (EDP). For PVADs (Jahren et al., 2014; Khir et al., 2006) and extra-aortic ACP devices (Campos Arias et al., 2017) similar waves have been reported. The hemodynamic effect of ACPs depends on the device synchronization and the interference between the device-generated and ventricular-generated waves (Sugawara et al., 2009).

The hemodynamic effect of DEAs has not been analyzed with WIA before. In our previous study (Martinez et al., 2022), the DEA was tested as an ACP *in-vivo* and for actuation at different time points (phase shifts (PS)) through the heart cycle. The best ACP result was achieved with an activation just before the start of systole and deactivation just after systole. The aim of the current study is to investigate the hemodynamic impact of the different PS on the WI. We hypothesize that the DEA-generated waves interfere with the ventricular-generated waves and that the wave's timing can be beneficial or detrimental to the device's performance.

2. Methods

Dielectric elastomer actuator. The DEA is a soft multilayer tube that replaces a section of the descending aorta. The positive electrode is encapsulated between two negative electrodes to confine the electrical field within the device, and the electrical connections are insulated to support voltages higher than 10 kV. The DEA is activated by applying a high voltage (<7kV). The DEAs are 40 or 50 mm long with 20 mm inner diameter. For detailed manufacturing process and geometry see (Martinez et al., 2022). Fig. 1A shows the DEA in activated (ON) and deactivated (OFF) states. When activated, the DEA diameter increases and sucks blood into the device, decreasing the pressure upstream and downstream of the device. When deactivated, the DEA diameter decreases and pushes blood out of the device, increasing the pressure upstream and downstream of the device. Fig. 1B shows the activation voltage signal used in this study.

Animals. This study has been approved by the Commission of Animal Experimentation of the Canton of Bern, Switzerland (Approval number BE14/2021). DEAs were implanted in five pigs (~50 kg) via left-sided thoracotomy. A section of the descending aorta was excised, and the DEA was anastomosed to the descending aorta. The heart rate was paced at 100 bpm using temporary pacemaker leads attached to the right atrium (Martinez et al., 2022). The first two animals were needed for training and tuning of the measurement protocol, while animal three died before any DEA could be tested. The final protocols and instrumentation were available in the last two animals.

Instrumentation. All recorded signals were acquired using Powerlab (ADInstruments, Houston, USA) and logged continuously (sampling frequency 1000 Hz) using LabChart Pro (ADInstruments, Houston, USA). The measured signals (see Fig. 1A) were LV pressure and volume (pressure–volume catheter, Millar, ADInstruments, Houston, USA), aortic pressure upstream and inside of the DEA (Xtrans, CODAN Pvb Critical Care GmbH, Forstinning, Germany), aortic flow upstream and downstream of the DEA (COnfidence, Transonic Systems, Inc., Ithaca, NY, USA), the pacemaker signal, and the DEA actuation voltage. The DEA was actuated using a high voltage unit (Trek 20/20C, Advanced Energy, Denver, USA) and a CompactDAQ (National Instruments, Austin, USA) connected to a computer with LabVIEW (National Instruments, Austin, USA).

Device synchronization. The peak of the pacemaker signal was used as actuation trigger; the computer-generated actuation signal was sent to the high voltage unit (Fig. 1B) and the DEA was actuated with well-defined delays after the trigger. The aortic valve opening (mid-point of LV pressure increase) was used as reference point for start of DEA actuation (defined as 0% of heart cycle). The actuation length (Fig. 1B) was set to the systolic length, measured as the time between aortic valve opening and closure (aortic flow-equivalent to dicrotic notch), and the rising and falling times were fixed at 50 ms. The time of aortic valve opening, and the systolic length were assumed to stay constant in each animal during pacing and were measured before the start of the protocols. See previous publication for further detail (Martinez et al., 2022).

Actuation protocols. The DEA actuation was delayed, or phase shifted (PS), compared to the aortic valve opening. The PS was varied from 0 to 90% in steps of 10% relative to the heart cycle length, giving a total of 10

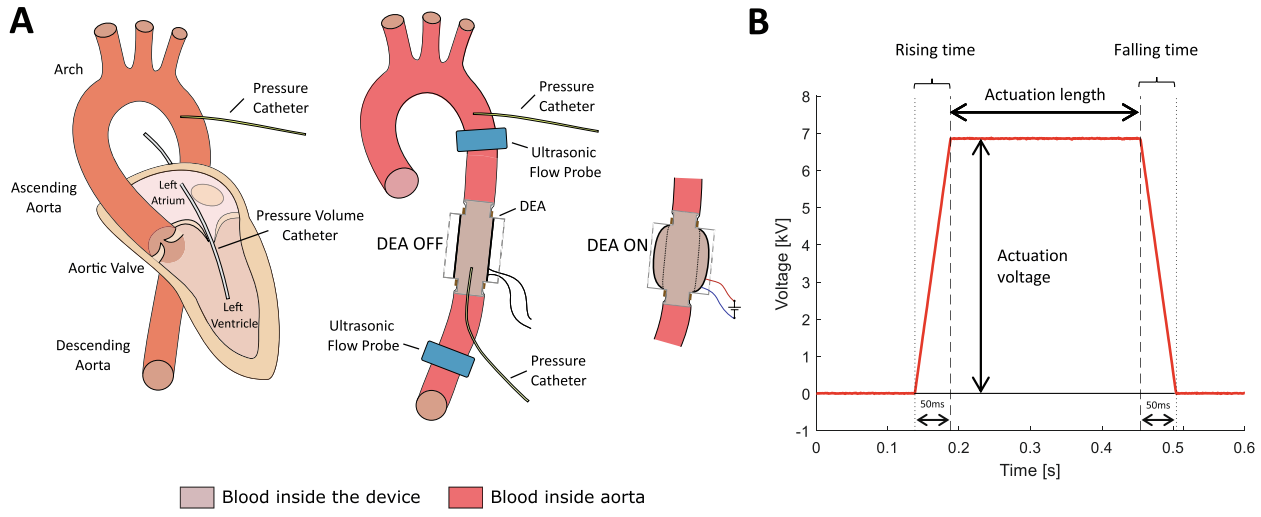

Fig. 1. A: Schematic of the DEA implantation in the descending aorta and the instrumentation (modified from (Martinez et al., 2022)). The DEA increases its internal diameter when activated (DEA ON) and returns to its passive state when deactivated (DEA OFF). B: The actuation voltage profile of the DEA.

PSs (Fig. 2A). To compensate for the time delay between the systolic pressure increase in the DEA compared to the LV (due to the distance), the DEA was actuated earlier (delay correction, Fig. 2B) to give time to the waves generated by the DEA to reach the aortic valve at the desired synchronization point. This delay was measured as the time between the mid-point of LV pressure increase and the foot of the pressure increase inside the DEA.

Each PS was maintained for 60 heart cycles. Baseline measurements (DEA off) were performed before and after each PS for at least 60 heart cycles. The actuation voltage was increased to 6–7 kV in steps of 0.5 kV leading to larger DEA deformation. The highest reached voltage level (before failing) was used in the analysis. Failing DEAs were replaced such that several DEAs were tested in each animal. Table 1 gives an overview of all animals, protocols, DEAs, and voltage levels used in the analysis.

Data processing and analysis. For each measurement, a stable interval consisting of 20 consecutive heart cycles (no arrhythmias, and stable pressure values) with DEA actuation and 20 consecutive baseline heart cycles were chosen. Hemodynamic parameters were calculated for each included heart cycle as well as the mean and standard deviation of each parameter. A single averaged heart cycle was calculated for the DEA-actuated and the baseline heart cycles.

The total WI was calculated as (Parker, 2009):

$$dI = dP \cdot dU$$

where I [W/m^2] is the total WI, P [Pa] is the aortic pressure, U [m/s] is the aortic blood flow velocity. dP and dU are the differences between two successive samples. U was estimated from the aortic flow (Q_{ao}) by assuming an inner aortic diameter of 10 mm with $U = Q_{ao}/A$, where A ([m^2]) is the aortic cross section. The P and Q_{ao} were assumed to be measured at the exact same location ($\sim$ 5 cmupstream of the DEA). Therefore, the flow and pressure were synchronized using the onset (foot) of the systolic pressure and flow increase at baseline. The WI was separated into its forward (+) and backward (−) components:

$$dP_{\pm} = \frac{1}{2}(dP \pm \rho c dU)$$

Table 1
Overview of animals and protocols used in the analysis. Several DEAs were implanted in each animal and tested for different voltage levels.

Animal	DEA	Length [mm]	Actuation voltage [kV]
4	1	29	7
	2	39	7
5	3	29	6.5
	4	39	6
	5	39	6.5

$$dU_{\pm} = \frac{1}{2}(dU \pm \frac{dP}{\rho c})$$

$$dI_{\pm} = dP_{\pm} \cdot dU_{\pm}$$

where ρ [kg/m^3] is the blood density (1060 kg/m^3) and c [m/s] is the wave speed. ρc was estimated from the linear slope of the P-U-loop at early systole (Khir et al., 2001b; Parker, 2009) at baseline. The forward and backward components were further decomposed into compression and decompression waves according to (Parker, 2009): Forward traveling waves means that $dI > 0$. A FCW corresponds to $dP > 0$ and $dU > 0$. A FDW corresponds to $dP < 0$ and $dU < 0$. Backward traveling waves means that $dI < 0$. A BCW corresponds to $dP > 0$ and $dU < 0$. A BDW corresponds to $dP < 0$ and $dU > 0$.

The EDP and the mean early diastolic pressure ($\overline{P_{\mathrm{dia}}}$) (calculated from end of systole to 150 ms before start of next systole) were calculated as measures for ACP efficiency. The hydraulic work (W_{H}[J]) in the aorta done by the heart (estimate of LV stroke work) was estimated by (Khir et al., 2001a; Kolyva et al., 2009):

$$W_{\mathrm{H}} = \int_0^T P \cdot Q_{\mathrm{ao}} \cdot dt$$

where T is the period of the heart cycle.

Statistics: The Wilcoxon rank sum test was used to assess if the DEA actuated heart cycles were significantly different to baseline for all parameters. A $p < 0.05$ was considered significant.

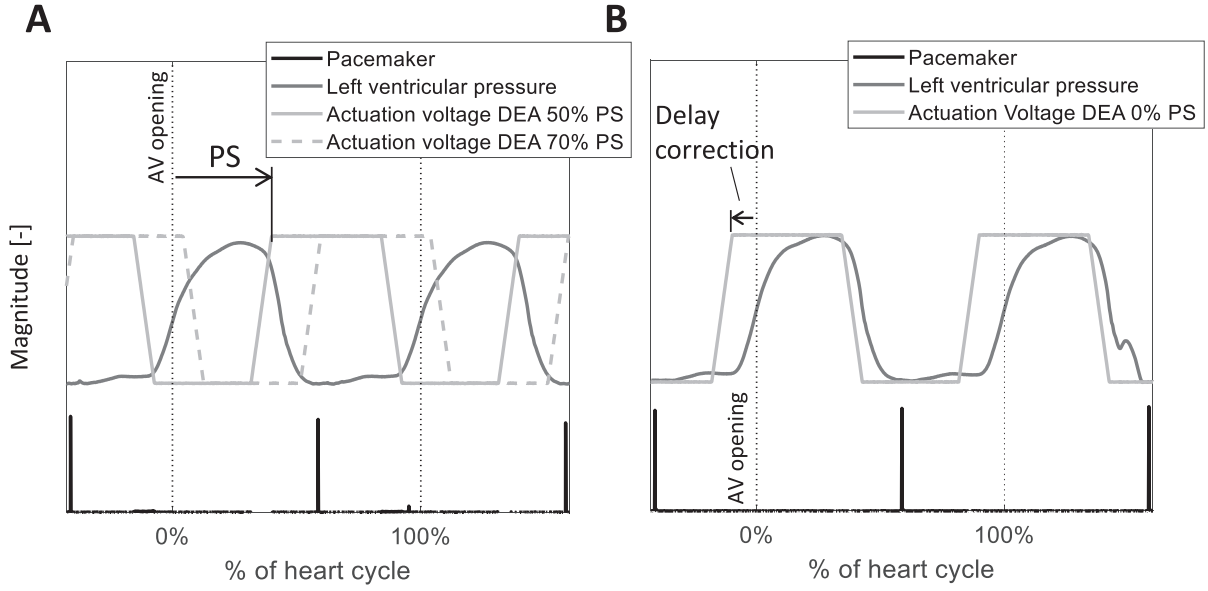

Fig. 2. (A). Left ventricular pressure and pacemaker signal together with DEA actuation signals for two different phase shifts (PS). PS is defined as the time between the start of DEA actuation and the aortic valve (AV) opening relative to the heart cycle in percentage. **B**: Left ventricular pressure and pacemaker signal together with DEA actuation signal for PS = 0% (at aortic valve opening). Delay correction: earlier DEA actuation to remove time delays in the pressure signal arising from the distance between the DEA and the left ventricle.

3. Results

The hemodynamic conditions varied during the experiments and among animals. Average mean arterial pressure was 63 ± 6 mmHg (52 −72 mmHg). Peak systolic pressure was 78 ± 6 mmHg (68 −89 mmHg). Wave speed was 1.07 ± 0.4 m/s (0.6 −1.9 m/s). Fig. 3A shows the averaged WI pattern for baseline and the total WI. The LV generated one FCW_{LV} and one FDW_{LV}, which were reflected (at the DEA) as BCW_{LV} and BDW_{LV}. Fig. 3B shows the corresponding pressure and velocity.

Fig. 3C and E show the averaged WI pattern seen for 0% and 50% PS compared to baseline. Fig. 3D and F show the corresponding pressure and velocity (see Supplementary Figs. 4 and 5 for consecutive beat to beat analysis). Upstream, the DEA generated a BDW_{DEA} at start of actuation and a BCW_{DEA} at the end of actuation traveling towards the heart. Downstream, forward waves were traveling towards the periphery (not further discussed in this study). The backward traveling waves reached the aortic valve and were reflected as FDW_{DEA} and FCW_{DEA}. At 0% PS (Fig. 3C), the reflected FDW_{DEA} was just ahead of aortic valve opening and the FCW_{LV}. The FCW_{LV} was larger and earlier than baseline. The reflected FCW_{DEA} arrived at end of systole and was partly superimposed to the FDW_{LV}. The FDW_{LV} was smaller and earlier than baseline. At 50% PS (Fig. 3E), the reflected FDW_{DEA} arrived at end of systole and was superimposed to the FDW_{LV}. The FDW_{LV} was larger and later than baseline. The reflected FCW_{DEA} arrived just before aortic valve opening and the FCW_{LV}. The FCW_{LV} was smaller and later than baseline.

Fig. 4 shows the WI pattern for baseline and the different PSs. The DEA-generated waves shift to the right for increasing PS and impact the LV-generated waves and the total WI pattern. Table 2 shows the average values, standard deviation, and significance of the FCW_{LV}'s and the FDW_{LV}'s peak values. The FCW_{LV} increased ($p < 0.05$) for 0, 20, 40, 60, and 80% PS with the largest increase at 60% PS, and decreased for 10, 30, and 50% PS with the largest decrease at 10% PS. The FDW_{LV} increased ($p < 0.05$) for 10, 50, 60, and 90% PS with the largest increase at 10% PS, and decreased for 0 and 40% PS with the largest decrease at 0% PS. Fig. 5 shows the average values for W_H, $\overline{P_{dia}}$, and EDP (average values, standard deviation and significance in Table 2). The W_H decreased for 0–20% and 80–90% PS ($p < 0.05$) and increased for 50–70% ($p < 0.05$). The $\overline{P_{dia}}$ increased for 0–20% PS ($p < 0.05$) and decreased for 30–70% PS ($p < 0.05$). The EDP decreased for 0% and 70–90% ($p < 0.05$) and increased for 20–50% PS ($p < 0.05$). The strongest ACP effect was seen in animal 4 DEA 2 (yellow line in Fig. 5) with augmentation of $\overline{P_{dia}}$ of 2% and decrease in EDP of 5–7%.

4. Discussion

In this study, wave intensity analysis (WIA) is performed for the first time to assess the hemodynamic effects of a soft, tubular dielectric elastomer actuator augmented aorta (DEA) implanted in porcine models (n = 2). DEAs were positioned in the descending aorta and actuated with ten different phase shifts (PS) in steps of 10%.

Actuating the DEA as an aortic counterpulsation (ACP) device (activation just before aortic valve opening (increase in diameter) and deactivation just after aortic valve closure (decrease in diameter)) gave the best overall results in terms of lower end-diastolic pressure (EDP) and augmented early diastolic pressure. This is in line with the optimal operation of intra-aortic balloon pumps (IABPs) (De Waha et al., 2014; Santa-Cruz et al., 2006). In comparison with IABPs, the non-obstructive DEAs can be actuated through the whole heart cycle without obstructing the flow. Moreover, the actuation time is much faster in a DEA (<20 ms (Martinez et al., 2022), current study 50 ms) than in IABPs (~200 ms), and actuation time is not affected by device angulation as in IABP (Bruti et al., 2015). This allows tuning of the DEA actuation timing to explore and optimize the assistance. WIA gives insight into the coupling between the device and the cardiovascular system and the interference between

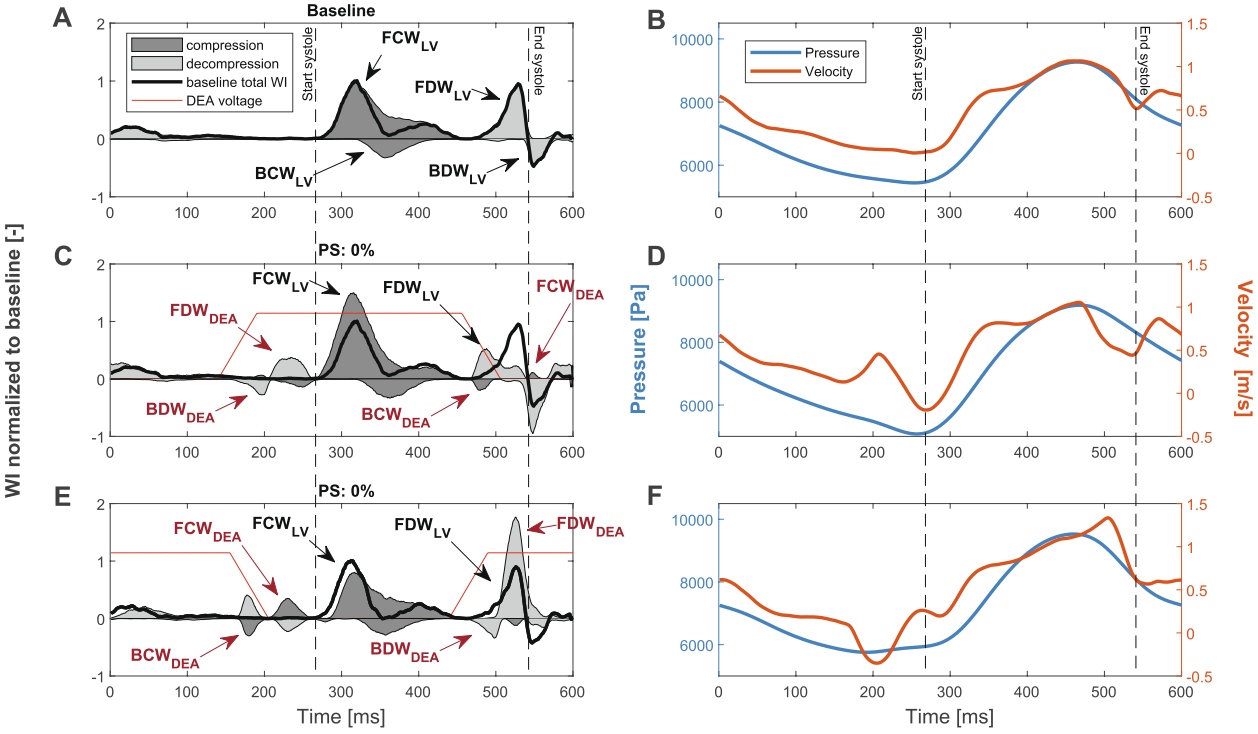

Fig. 3. Wave intensity (WI) pattern for baseline (**A**), DEA activation with phaseshift (PS) 0% (**C**) and 50% (**E**) seen in animal 4 DEA 2 at 7 kV for the averaged heart cycle decomposed into forward and backward compression and decompression, and baseline total WI. The corresponding pressure and velocity (**B**, **D**, **F**) waveforms for the averaged heart cycle. The WI is normalized to the baseline peak value of the forward compression wave of the left ventricle (FCW_{LV}). The vertical dashed lines mark the start of systole (onset of FCW_{LV} in baseline at the measurement site), and the end of systole (end of FDW_{LV} in baseline at the measurement site), respectively. FDW: forward decompression wave, FCW: forward compression wave, BDW: backward decompression wave, BCW: backward compression wave, LV: left ventricle. DEA: dielectric elastomer actuator, WI: wave intensity.

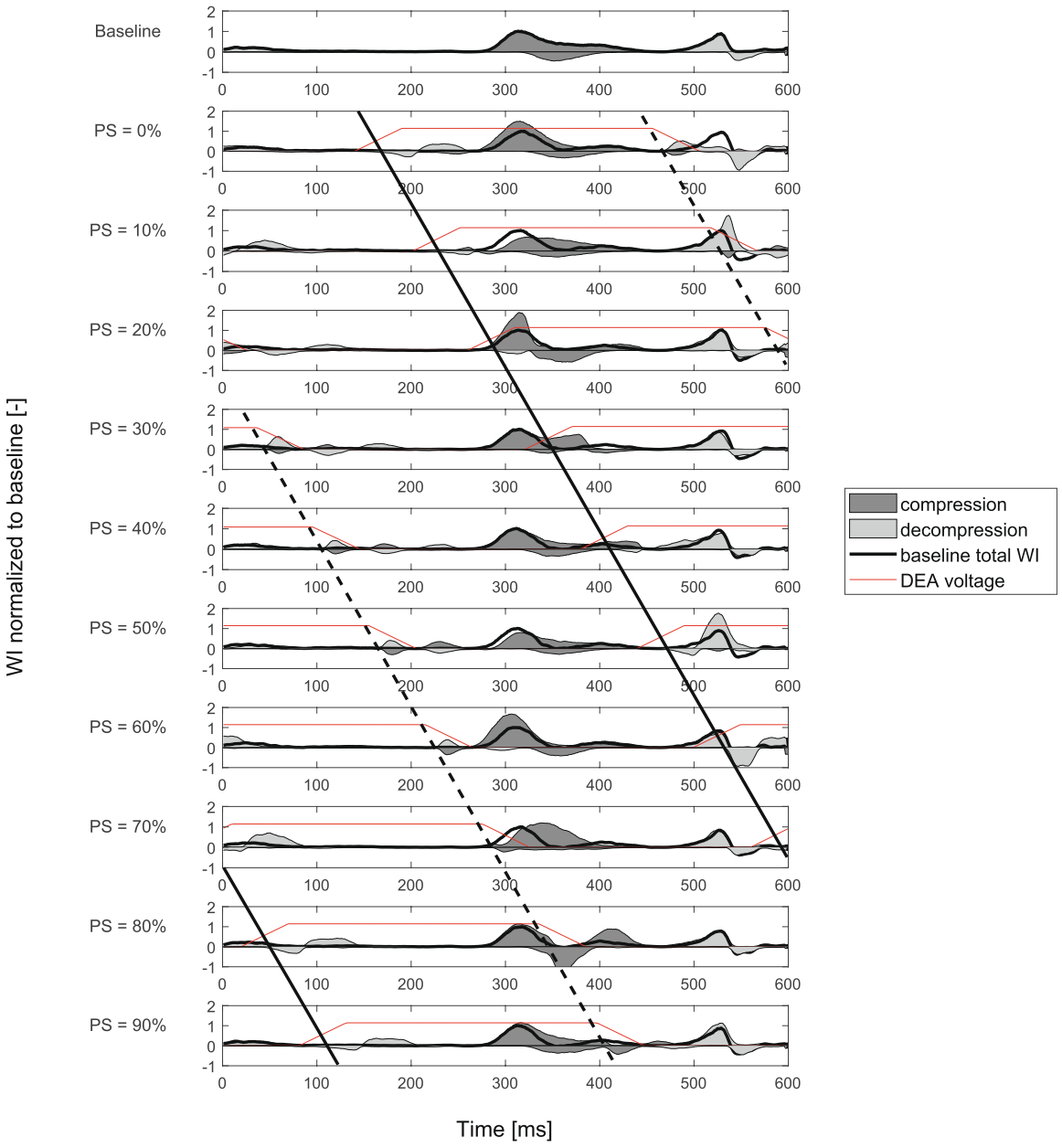

Fig. 4. WI pattern normalized to the peak value of the baseline forward compression wave seen in animal 4, DEA 2 for baseline and the 10 different phase shifts. The black solid lines indicate the DEA backward decompression wave generated by DEA activation and the dotted black lines indicate the DEA backward compression wave generated by the DEA deactivation. PS: phase shift. DEA: dielectric elastomer actuator. WI: wave intensity.

Table 2
Average values and standard deviation of the peak values of the left ventricular forward compression and decompression waves, hydraulic work, mean early diastolic pressure and EDP in % change compared to baseline for the different phase shifts for all animals and DEAs.

	Phase shift [% of heart cycle]									
	0	10	20	30	40	50	60	70	80	90
FCW_{LV}	26 ± 15*	−27 ± 8.8*	41 ± 18*	−6.1 ± 6.8*	8.3 ± 8.8*	−24 ± 6.1*	60 ± 16*	−4.8 ± 17	6.3 ± 6.0*	1.5 ± 8.5
FDW_{LV}	−42 ± 11*	59 ± 20*	0.6 ± 11	1.5 ± 13	−8.5 ± 10*	27 ± 31*	24 ± 42*	4.0 ± 13	−1.7 ± 13	20 ± 11*
W_H	−1.4 ± 2.5*	−1.1 ± 2.7*	−1.1 ± 2.6*	0.0 ± 2.5	0.5 ± 2.8	2.3 ± 3.1*	1.1 ± 2.6*	0.6 ± 2.5*	−0.6 ± 2.5*	−1.7 ± 2.5*
$\overline{P_{dia}}$	1.1 ± 1.1*	1.3 ± 1.1*	0.7 ± 1.3*	−0.2 ± 1.0*	−0.8 ± 1.0*	−0.5 ± 1.8	−0.8 ± 0.9*	−1.0 ± 1.0*	0.1 ± 1.1	0.3 ± 1.0
EDP	−3.0 ± 2.2*	−0.1 ± 0.7	0.9 ± 1.1*	1.0 ± 1.0*	1.3 ± 0.9*	3.4 ± 1.6*	−0.2 ± 0.7	−0.9 ± 0.7*	−0.9 ± 1.0*	−2.2 ± 2.1*

FCW: forward compression wave. FDW: forward decompression wave. LV: left ventricle. W_H: hydraulic work.
$\overline{P_{dia}}$: mean early diastolic pressure. EDP: end-diastolic pressure.
*Significant different from baseline ($p < 0.05$).

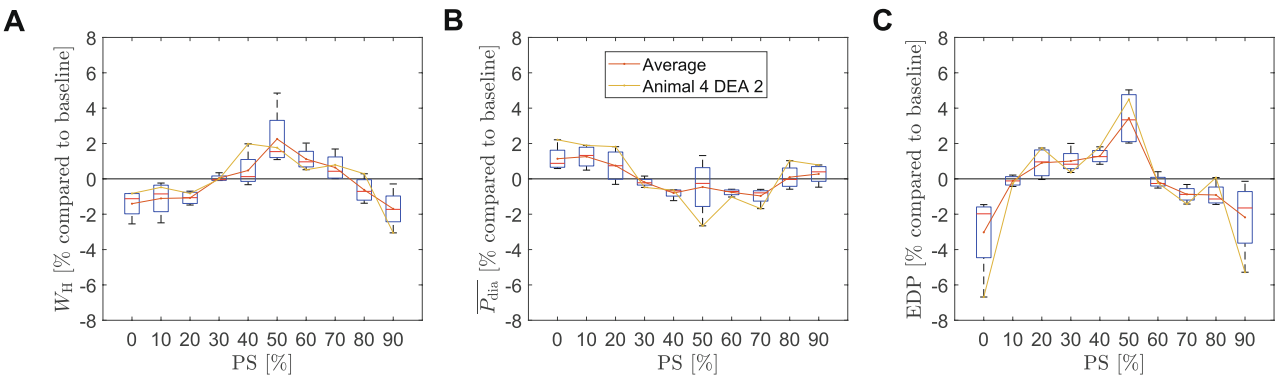

Fig. 5. Average values for the (**A**) hydraulic work (W_H), the (**B**) mean diastolic pressure ($\overline{P_{dia}}$) and the (**C**) end diastolic pressure (EDP) compared to baseline for all phase shifts (PS) for all animals and DEAs. The values are represented in boxplots in which the red lines represent the median value, and the edges of the boxes represent the 25th and 75th percentile, respectively. The average value for all animals and DEA is shown in red, and the results of animal 4 DEA 2 showing the strongest impact on EDP and $\overline{P_{dia}}$ is shown in yellow. (For interpretation of the references to colour in this figure legend, the reader is referred to the web version of this article.)

waves. In the present study, we hypothesized that the DEA actuation timing changes the wave intensity (WI) pattern, and we used WIA to assess whether the timing of the DEA-generated waves can be beneficial or detrimental for the cardiovascular system.

The baseline WI (Fig. 3A) consisted of one forward compression wave (FCW) and one forward decompression wave (FDW) generated by the LV in line with (Khir et al., 2001b; Parker, 2009). The FCW_{LV}'s peak value has been linked to cardiac contractility, with a larger peak value indicating higher LV contractility (Sugawara et al., 2009). The physiological meaning of the FDW_{LV} is more complex. A decrease in the peak value can be due to a decline in the cardiac muscle tension bearing ability or to a change in the inertial force of the aortic blood flow, or both (Sugawara et al., 2009). The DEA introduces two pairs of new waves (Fig. 3C and E): one backward decompression wave (BDW_{DEA}) together with the corresponding reflected FDW_{DEA} at activation and one backward compression wave (BCW_{DEA}) together with the corresponding reflected FCW_{DEA} at deactivation (The reflection coefficient at the aortic valve seems to be positive for all PS). These DEA-generated waves are similar to waves generated by other ACP devices and pulsatile ventricular assist devices (Campos Arias et al., 2017; Jahren et al., 2014; Khir et al., 2006; Kolyva et al., 2009; Lu et al., 2012). However, the waves of the IABP (Kolyva et al., 2009; Lu et al., 2012) are larger (relative peak values) compared to the DEA-generated waves. This is expected, due to the large volume displacement of the IABP (up to 50 cm^3) compared to the small of the DEA (<2 cm^3) and that the DEA does not obstruct the aortic lumen.

The DEA-generated waves interfere differently with the LV-generated waves depending on the PS (Fig. 3 and Fig. 4). For 0% PS (Fig. 3C), the BDW_{DEA} (DEA activation) reaches the aortic valve just before opening, and lowers the EDP (Fig. 5C). This leads to a larger and faster FCW_{LV} compared to baseline, indicating a stronger LV ejection in line with (Sugawara et al., 2009). A similar increase in FCW_{LV} was also observed by (Lu et al., 2012) in response to IABP deflation. The BCW_{DEA} (DEA deactivation) arrives at the same time as the start of the FDW_{LV}. The corresponding reflected FCW_{DEA} and the FDW_{LV} superimpose, and the FDW_{LV} peak decreases and occurs earlier. The hemodynamic effect of this interference is unclear. It could indicate a reduction in the inertial force of the blood flow out of the LV (Sugawara et al., 2009) which might lead to an earlier closure of the aortic valve and interfere with the total load on the LV. For 0% PS, the DEA reduces the hydraulic work (W_H) and thereby unloads the LV. This is in line with the reduced EDP, and with the possible earlier valve closure. For 50% PS (Fig. 3E), the BCW_{DEA} arrives just before aortic valve opening, and increases EDP (Fig. 5C). This leads to a lower and delayed FCW_{LV} indicating a weaker LV ejection in line with (Sugawara et al., 2009). The BDW_{DEA} arrives just before aortic valve closure and delays the FDW_{LV} compared to baseline. The corresponding reflected FDW_{DEA} superimposes with the FDW_{LV}, and the peak of the FDW_{LV} increases. A stronger FDW_{LV} could indicate an increased inertial force of the blood flow and thereby a delay in valve closure. For 50% PS, the DEA increased W_H, leading to increased LV load. This is in line with the increased EDP and the delayed FDW_{LV}. The wave interferences differ for all PS. For 60% PS, the DEA increases the FCW_{LV} the most. Here the reflected FCW_{DEA} superimposes with the FCW_{LV} and increases the W_H, leading to increased LV load. Fine-tuning of the start and end of actuation could optimize the effect of the DEA on the different hemodynamic parameters and the load of the heart (see Supplementary Materials). This finding is in line with (Lu et al., 2012), who observed improved efficiency of IABPs and para-aortic ACP devices depending on the wave timing.

The intended use of the DEA is as an ACP device. The non-obstructive nature of the DEA (aortic lumen open at all times, even at electrical failure) and the pure electrical actuation are advantages compared to current ACPs (De Waha et al., 2014; Khan et al., 2023; Santa-Cruz et al., 2006), and could enable a fully implantable device, for medium to long-term use. For a future final medical device, a modified design wrapping around the aorta would be desirable to reduce the invasiveness of the implantation and keep the native aorta intact. The effect of the device in the current study is modest (1–6%) but is expected to be higher in stiffer aortas (ageing) and in patients with hypertension. Higher pressures would generate larger deformations of the DEA and larger displaced volumes. The damping of the aortic waves is less in a stiffer system and the pulse wave velocity is higher. Optimization of the design is expected to further improve the effectiveness of the DEA.

Limitations: The acute experiments affected the pig's hemodynamics leading to lower aortic pressure and flow. An implantation in the human ascending aorta is expected to further improve the DEA efficiency (Sales and McCarthy, 2010). The small number (n = 2) of animals is a drawback. However, five different DEAs were tested, and many actuation cycles (3000 cycles (+2700 in the Supplementary materials)) were performed. WIA depends on pressure and velocity measurements in the same location. Although we aimed to position the flow and pressure sensors in the same location, the final exact position of the pressure sensor was difficult to assess. This might have contributed to the large variation seen in the estimated wave speeds. This, however, did not change the qualitative findings of the WIA between the different measurements. Additionally, WIA in the intact aorta could not be provided, this will be implemented in the future.

5. Conclusion

The wave intensity analysis shows that the DEA generated similar waves as other ACPs, and that the timing of these waves affected the

DEA's efficacy. The non-obstructive nature of the DEA allowed to phase shift the device actuation throughout the full heart cycle, and we show that the DEA-generated waves were shifted and interfered differently with the ventricular-generated waves. The wave interference gave insight into why the actuation time was beneficial or detrimental for the cardiac load. The best actuation timing led to decreased hydraulic work and end-diastolic pressure, and an augmented early diastolic pressure.

Funding

The authors declare that the study was supported by the Werner Siemens Stiftung, Zug, Switzerland received by Yves Perriard.

Grants

This study was supported by the Werner Siemens Stiftung, Zug, Switzerland.

CRediT authorship contribution statement

Silje Ekroll Jahren: Conceptualization, Methodology, Investigation, Formal analysis, Data curation, Validation, Writing – original draft, Visualization, Writing – review & editing. **Thomas Martinez:** Writing – review & editing, Validation, Methodology, Investigation, Formal analysis, Data curation, Conceptualization. **Armando Walter:** Writing – review & editing, Methodology, Investigation. **Lorenzo Ferrari:** Writing – review & editing, Investigation, Formal analysis, Data curation. **Francesco Clavica:** Writing – review & editing, Validation, Methodology, Investigation, Conceptualization. **Dominik Obrist:** Writing – review & editing, Validation, Supervision, Resources, Methodology, Conceptualization. **Yoan Civet:** Writing – review & editing, Validation, Supervision, Resources, Methodology, Investigation, Funding acquisition, Conceptualization. **Yves Perriard:** Writing – review & editing, Supervision, Resources, Project administration, Methodology, Funding acquisition, Conceptualization.

Declaration of Competing Interest

The authors declare that they have no known competing financial interests or personal relationships that could have appeared to influence the work reported in this paper.

Acknowledgments

We would like to thank the Werner Siemens Stiftung, which funded and supported this study. We would further like to thank Paul Philipp Heinisch for performing the main surgery and the experimental surgery facility team of the University of Bern (Daniela Casoni, Kay Nettelbeck, Luisana Garcia, Angela Wicki, MariaFrancesca Petrucci), Maks Mihalj, Andreas Häberlin and Hansjörg Jenni for assistance before and during the *in-vivo* experiments.

Appendix A. Supplementary data

Supplementary data to this article can be found online at https://doi.org/10.1016/j.jbiomech.2023.111777.

References

Almanza, M., Clavica, F., Chavanne, J., Moser, D., Obrist, D., Carrel, T., Civet, Y., Perriard, Y., 2021. Feasibility of a dielectric elastomer augmented aorta. Adv. Sci. 8, 2001974. https://doi.org/10.1002/advs.202001974.

Bruti, G., Kolyva, C., Pepper, J.R., Khir, A.W., 2015. Measurements of intra-aortic balloon wall movement during inflation and deflation: effects of angulation. E154–E163 Artif. Organs 39. https://doi.org/10.1111/AOR.12509.

Campos Arias, D., Londono, F., Rodríguez Moliner, T., Georgakopoulos, D., Stergiopulos, N., Segers, P., 2017. Hemodynamic impact of the C-pulse cardiac support device: a one-dimensional arterial model study. E141–E154 Artif. Organs 41. https://doi.org/10.1111/aor.12922.

Davies, A.N., Peters, W.S., Su, T., Sullivan, C.E., Perkidides, T., Milsom, F.P., White, G., 2005. Extra-ascending aortic versus intra-descending aortic balloon counterpulsation - effect on coronary artery blood flow. Hear. Lung Circ. 14, 178–186. https://doi.org/10.1016/j.hlc.2005.03.018.

De Waha, S., Desch, S., Eitel, I., Fuernau, G., Lurz, P., Sandri, M., Schuler, G., Thiele, H., 2014. Intra-aortic balloon counterpulsation — basic principles and clinical evidence. Vasc.Pharmacol. 60, 52–56. https://doi.org/10.1016/J.VPH.2013.12.003.

Jahren, S.E., Amacher, R., Weber, A., Most, H., Flammer, S.A., Traupe, T., Stoller, M., de Marchi, S., Vandenberghe, S., 2014. Effects of Thoratec pulsatile ventricular assist device timing on the abdominal aortic wave intensity pattern. H1243–H1251 Am. J. Physiol. Circ. Physiol. 307. https://doi.org/10.1152/ajpheart.00085.2014.

Khan, T., Ashraf, T., Roomi, F., 2023. The effect of intra-aortic balloon pump in patients with low ejection fraction undergoing coronary artery bypass grafting. Biol. Clin. Sci. Res. J. 2023, 214 https://doi.org/10.54112/bcsrj.v2023i1.214.

Khir, A.W., Henein, M.Y., Koh, T., Das, S.K., Parker, K.H., Gibson, D.G., 2001a. Arterial waves in humans during peripheral vascular surgery. Clin. Sci. 101, 749. https://doi.org/10.1042/CS20010046.

Khir, A.W., O'Brien, A., Gibbs, J.S.R., Parker, K.H., 2001b. Determination of wave speed and wave separation in the arteries. J. Biomech. 34, 1145–1155. https://doi.org/10.1016/S0021-9290(01)00076-8.

Khir, A.W., Swalen, M.J., Segers, P., Verdonck, P., Pepper, J.R., 2006. Hemodynamics of a pulsatile left ventricular assist device driven by a counterpulsation pump in a mock circulation. Artif. Organs 30, 308–312. https://doi.org/10.1111/j.1525-1594.2006.00218.x.

Knecht, O., Bosshard, R., Kolar, J.W., 2015. High-efficiency transcutaneous energy transfer for implantable mechanical heart support systems. IEEE Trans. Power Electron. 30, 6221–6236. https://doi.org/10.1109/TPEL.2015.2396194.

Kolyva, C., Pantalos, G.M., Giridharan, G.A., Pepper, J.R., Khir, A.W., 2009. Discerning aortic waves during intra-aortic balloon pumping and their relation to benefits of counterpulsation in humans. J. Appl. Physiol. 107, 1497–1503. https://doi.org/10.1152/japplphysiol.00413.2009.

Lu, P.-J., Lin, P.-Y., Yang, C.-F.-J., Hung, C.-H., Chan, M.-Y., Hsu, T.-C., 2011. Hemodynamic and metabolic effects of para- versus intraaortic counterpulsatile circulation supports. ASAIO J. 57, 19–25. https://doi.org/10.1097/MAT.0b013e3181fcbc7d.

Lu, P.-J., Yang, C.-F.-J., Wu, M.-Y., Hung, C.-H., Chan, M.-Y., Hsu, T.-C., 2012. Wave intensity analysis of para-aortic counterpulsation. H1481–H1491 Am. J. Physiol. Circ. Physiol. 302. https://doi.org/10.1152/ajpheart.00551.2011.

Martinez, T., Jahren, S.E., Walter, A., Chavanne, J., Clavica, F., Ferrari, L., Heinisch, P.P., Casoni, D., Haeberlin, A., Luedi, M.M., Obrist, D., Carrel, T., Civet, Y., Perriard, Y., 2022. A novel soft cardiac assist device based on a dielectric elastomer augmented aorta: an in vivo study. Transl. Med. Bioeng. https://doi.org/10.1002/btm2.10396.

Parker, K.H., 2009. An introduction to wave intensity analysis. Med. Biol. Eng. Compu. 47, 175–188. https://doi.org/10.1007/s11517-009-0439-y.

Pelrine, R., Kornbluh, R., Joseph, J., Heydt, R., Pei, Q., Chiba, S., 2000. High-field deformation of elastomeric dielectrics for actuators. Mater. Sci. Eng. C 11, 89–100. https://doi.org/10.1016/S0928-4931(00)00128-4.

Penny, D.J., Mynard, J.P., Smolich, J.J., 2008. Aortic wave intensity analysis of ventricular-vascular interaction during incremental dobutamine infusion in adult sheep. Am. J. Physiol. - Hear. Circ. Physiol. 294, 481–489. https://doi.org/10.1152/AJPHEART.00962.2006.

Redheuil, A., Yu, W.C., Wu, C.O., Mousseaux, E., De Cesare, A., Yan, R., Kachenoura, N., Bluemke, D., Lima, J.A.C., 2010. Reduced ascending aortic strain and distensibility: earliest manifestations of vascular aging in humans. Hypertension 55, 319–326. https://doi.org/10.1161/HYPERTENSIONAHA.109.141275.

Sales, V.L., McCarthy, P.M., 2010. Understanding the C-pulse device and its potential to treat heart failure. Curr. Heart Fail. Rep. 7, 27–34. https://doi.org/10.1007/s11897-010-0007-7.

Santa-Cruz, R.A., Cohen, M.G., Ohman, E.M., 2006. Aortic counterpulsation: a review of the hemodynamic effects and indications for use. Catheter. Cardiovasc. Interv. 67, 68–77. https://doi.org/10.1002/ccd.20552.

Sugawara, M., Niki, K., Ohte, N., Okada, T., Harada, A., 2009. Clinical usefulness of wave intensity analysis. Med. Biol. Eng. Compu. 47, 197–206. https://doi.org/10.1007/s11517-008-0388-x.

Sun, Y.H., Anderson, T.J., Parker, K.H., Tyberg, J.V., 2000. Wave-intensity analysis: a new approach to coronary hemodynamics. J. Appl. Physiol. 89, 1636–1644. https://doi.org/10.1152/JAPPL.2000.89.4.1636.